Nationaal Lucht- en Ruimtevaartlaboratorium
National Aerospace Laboratory NLR

NLR-TP-2001-141

Eigenvalues and eigenfunctions of ducted swirling flows

R.J. Nijboer

Nationaal Lucht- en Ruimtevaartlaboratorium
National Aerospace Laboratory NLR

NLR-TP-2001-141

Eigenvalues and eigenfunctions of ducted swirling flows

R.J. Nijboer

This report is based on a presentation held at the 7th AIAA/CEAS Aeroacoustics Conference, Maastricht, The Netherlands, 28-30 May 2001.

Division:	Fluid Dynamics
Issued:	27 March 2001
Classification of title:	Unclassified

Contents

8 Figures

(16 pages in total)

List of symbols

J_m	mth-order Bessel function of the first kind
M	axial Mach number
m	circumferential harmonic
N	number of grid points
p	pressure (perturbation)
r, θ, x, t	cylindrical co-ordinates
s	radial co-ordinate near the critical layer
u_r, u_θ, u_x	perturbed velocity components
V_θ, V_x	mean velocity components
$\vec{v}$	velocity vector
Y_m	mth-order Bessel function of the second kind
Z	acoustic impedance
α	axial wave number
Γ	free-vortex swirl strength
γ	specific heat ratio (= 1.4)
ε	solid-block swirl strength (small)
λ	radial wave number
ρ	density (perturbation)
Ω	solid-block swirl strength
ω	frequency

subscript:

0	mean flow property
c	at the critical layer

superscript:

~	transformed variable

AIAA 2001-2178

EIGENVALUES AND EIGENFUNCTIONS OF DUCTED SWIRLING FLOWS

Ronald Nijboer*
National Aerospace Laboratory NLR, 8300 AD Emmeloord, The Netherlands

Abstract

A numerical method using finite elements for the solution of the eigenvalues and eigenfunctions in non-uniform, non-axial ducted flows is described. The method is validated against results from the literature for swirling flows and against an approximate analytical solution for a small solid block swirl. In non-uniform flows not only acoustic modes are present, but also hydrodynamic modes, instabilities, and continuum modes may occur. The continuum modes and hydrodynamic modes are analysed. A necessary condition for the existence of hydrodynamic modes is derived.

Introduction

One of the major noise sources of modern turbofan engines is the rotor-stator interaction noise. In order to be able to design more quiet engines it is important to have a good understanding of the noise mechanism and to have the tools to compute the noise source and the propagation of the noise. The mechanism for rotor-stator interaction noise is the impinging on the stator vanes of wakes coming from the rotor blades. On the vanes the wakes induce unsteady loading which generates sound waves travelling both in upstream and in downstream direction. The downstream propagating sound waves travel either through the engine core or the by-pass duct. The upstream propagating sound waves travel towards the rotor, where they are partly reflected and partly transmitted. The transmitted part propagates forward into the intake.

In order to calculate the forward radiating sound it is important to accurately describe the propagation of disturbances in the region between rotor and stator. The propagation of disturbances in this region is rather complicated due to the splitter and the swirling flow. The problem of diffraction of sound by the splitter in uniform flows is considered in, for instance, reference 1. Here we address the problem of propagation of disturbances in a hard walled annular duct with constant radius containing a swirling flow.

Sound propagating in a duct with uniform flow can be described by modes. These modes can be found by solving the convected wave equation for the perturbed pressure as an eigenvalue problem for the axial wave number. This problem has two sets of discrete eigenvalues as solution: one set of downstream propagating acoustic modes and one set of upstream propagating acoustic modes. The eigenfunctions corresponding to these eigenvalues form a complete, orthogonal set and, hence, every pressure perturbation can be described by a combination of these eigenfunctions.[2]

When the flow is not uniform anymore, but contains e.g. swirl or axial shear, it is still possible to use a description of modes. However, the set of eigenfunctions corresponding to the acoustic modes (pressure dominated) is not complete and not orthogonal anymore. Instead, additional hydrodynamic modes (velocity dominated; also called 'nearly convected' modes) and / or instabilities may arise.[3] Also a continuum of eigenvalues may be present. Whereas the discrete modes have regular eigenfunctions both in Fourier space and in physical space, the continuous modes have eigenfunctions that are irregular in Fourier space and correspond to algebraically growing or decaying modes in physical space.[4, 5, 6]

In order to investigate the effect of flow non-uniformity on the propagation of disturbances a method was developed to calculate the eigenvalues and eigenfunctions of disturbances in a hard walled cylindrical or annular duct containing arbitrary

* Research Engineer, Aeroacoustics Department,
P.O. Box 153, e-mail: nijboer@nlr.nl.

flow. The eigenfunctions are discretised using finite elements. Application of the Galerkin method then leads to an eigenvalue problem for the axial wave number that is solved using standard numerical techniques.

In order to validate the method it was checked against swirling flow results available in the literature. Kousen[7, 8] and Golubev & Atassi[9] developed programs based on similar methods as ours. Their methods are based on the assumption of a homentropic flow, whereas this limitation is not made here. Tam & Auriault[10] used a different method. We will compare our results against those of Kousen and Tam & Auriault.

Since swirling flow data is not widely available in the literature, an approximate analytical solution was constructed for a small solid block swirl. In this way the numerical method was further validated.
As mentioned before, the complete spectrum for a non-uniform flow may consist of acoustic modes, hydrodynamic modes, instabilities, and continuum modes. The continuum modes and the hydrodynamic modes will be considered in more detail. The local behaviour of the singular continuum modes is described and a condition for the existence of the hydrodynamic modes is derived.

Flow model

The flow of an ideal, inviscid gas in an annular or cylindrical duct can be described by the equations for mass continuity,

$$\frac{\partial \rho}{\partial t} + \nabla \cdot (\rho \vec{v}) = 0, \tag{1}$$

for momentum,

$$\rho \frac{\mathrm{D}\vec{v}}{\mathrm{D}t} + \nabla p = 0\,, \tag{2}$$

and for internal energy, expressed in terms of pressure evolution,

$$\frac{\mathrm{D}p}{\mathrm{D}t} + \gamma p \nabla \cdot \vec{v} = 0\,. \tag{3}$$

Here ρ denotes density, $\vec{v}$ denotes the velocity vector, p denotes pressure, γ denotes the specific heat ratio (which is taken 1.4), and

$$\frac{\mathrm{D}}{\mathrm{D}t} = \frac{\partial}{\partial t} + \vec{v} \cdot \nabla \tag{4}$$

is the convective derivative.

When the duct has constant radius, the mean flow satisfying equations (1) – (3) takes the form

$$\rho = \rho_0(r), \quad \vec{v} = V_\theta(r)\vec{e}_\theta + V_x(r)\vec{e}_x\,. \tag{5}$$

These radial profiles are free to choose. The mean pressure, p_0, then follows from force balance

$$\frac{\mathrm{d}p_0}{\mathrm{d}r} = \frac{\rho_0 V_\theta^2}{r}\,. \tag{6}$$

Note that we did not make the assumption of a homentropic (i.e. uniform entropy) flow. For such a flow holds

$$\frac{\mathrm{d}p_0}{\mathrm{d}r} = \frac{\gamma p_0}{\rho_0}\frac{\mathrm{d}\rho_0}{\mathrm{d}r}\,. \tag{7}$$

Then equations (6) and (7) determine both the mean pressure and the mean density for a given swirl distribution, whereas for non-homentropic flows only the pressure is determined. We emphasise this, because an unfavourable density distribution may yield an unstable flow.

In order to describe the disturbances on the mean flow, equations (1) – (3) are linearised. The subscript '0' is used to denote the mean density and mean pressure distribution, whereas the symbols without subscript will now denote the perturbed density and pressure. The perturbed velocity is denoted by u_r, u_θ and u_x . Also all variables are scaled by the (constant) duct outer radius, the mean density at the duct outer radius, and the speed of sound at the duct outer radius. Finally, we assume that the disturbances have an exponential dependence like

$$f(r,\theta,x,t) = f(r)\exp(im\theta + i\alpha x + i\omega t)\,. \tag{8}$$

When the mean flow is described and the circumferential mode number, m, and the time harmonic, ω, are given, then the linearised flow equations yield an eigenvalue problem for the axial wave number α. For simple mean flows this eigenvalue problem can be solved analytically, as done for a uniform flow by Tyler and Sofrin.[2] For more complex mean flows, however, numerical methods have to be used.

Numerical method

For the numerical solution of the eigenvalue problem the following transformation is applied

$$\begin{aligned} &\tilde{\rho} = r\rho, \quad \tilde{p} = rp, \\ &\tilde{u}_r = -iru_r, \quad \tilde{u}_\theta = u_\theta, \quad \tilde{u}_x = ru_x. \end{aligned} \tag{9}$$

Using equations (8) and (9), the linearised version of equations (1) – (3) can be written as

$$\begin{aligned} \alpha\left(V_x\tilde{\rho} + \rho_0\tilde{u}_x\right)/r &= -\left(\omega + mV_\theta/r\right)\tilde{\rho} - \rho_0'\tilde{u}_r/r \\ &\quad - \rho_0\left(\tilde{u}_r' + m\tilde{u}_\theta\right)/r, \\ \alpha\rho_0 V_x\tilde{u}_r &= -\rho_0\left(\omega + mV_\theta/r\right)\tilde{u}_r + r\left(\tilde{p}/r\right)' \\ &\quad - 2\rho_0 V_\theta\tilde{u}_\theta - V_\theta^2\tilde{\rho}/r, \\ \alpha r\rho_0 V_x\tilde{u}_\theta &= -r\rho_0\left(\omega + mV_\theta/r\right)\tilde{u}_\theta - m\tilde{p}/r \\ &\quad - \rho_0\left(V_\theta' + V_\theta/r\right)\tilde{u}_r, \\ \alpha\left(\rho_0 V_x\tilde{u}_x + \tilde{p}\right)/r &= -\rho_0\left(\omega + mV_\theta/r\right)\tilde{u}_x/r \\ &\quad - \rho_0 V_x'\tilde{u}_r/r, \\ \alpha\left(\gamma p_0\tilde{u}_x + V_x\tilde{p}\right)/r &= -\left(\omega + mV_\theta/r\right)\tilde{p}/r - p_0'\tilde{u}_r/r \\ &\quad - \gamma p_0\left(\tilde{u}_r' + m\tilde{u}_\theta\right)/r. \end{aligned} \tag{10}$$

Here a prime denotes the derivative with respect to radius. Note that due to the transformation (9) the set of equations (10) has real coefficients.

The set of equations (10) is completed with boundary conditions. For acoustically soft walls the boundary condition at the wall reads[11]

$$n\omega\tilde{u}_r = \left(\omega + \frac{mV_\theta}{r} + \alpha V_z\right)\tilde{p}/Z, \tag{11}$$

where $n = +1$ at the duct outer radius, and $n = -1$ at the hub. Z is the acoustic impedance of the wall. For a circular geometry (no hub) the solution is assumed to be regular at the centre:

$$\tilde{u}_r = 0. \tag{12}$$

In the present paper we restrict ourselves to hard walled ducts. Hence condition (11) can be replaced by condition (12) at the duct outer radius and at the hub.

Equations (10) combined with the boundary conditions define an eigenvalue problem for α. The solution of this problem can be approximated using the finite element Galerkin method. Multiplying the equations with test functions and integrating over the radial domain yields a weak solution to the problem.

As test functions two types of local functions are used, a set of cubic splines to represent the radial velocity perturbation and its derivative and a set of quadratic elements to represent the other perturbations, see Figure 1. Using third and second order elements, allows for the accurate solution of the divergence of the perturbed velocity. This method was originally used to find the magneto-hydrodynamic spectrum of static plasmas[12] and more recently it was extended to allow for flowing plasmas.[13] It was found that the use of n+1-th order and n-th order elements eliminates spurious modes that arise due to coupling of different types of waves.[12]

After discretisation equations (10) can be written in matrix form

$$A\vec{x} = \alpha B\vec{x}. \tag{13}$$

Due to the local basis functions the matrices A and B have block tri-diagonal form. Two basis functions are used per grid point (Figure 1), hence the matrices have dimension $2\times5\times N$ by $2\times5\times N$, where N is the number of grid points.

The block tri-diagonal form of the matrices can be exploited by using an iterative solution method. The advantage of such a method is that it allows for

a fast solution of part of the spectrum using a large number of grid points. The disadvantage is that only one or a few eigenvalues will be found. Therefore, we opted for a standard QR solver to calculate the complete spectrum for a relatively low number of grid points. For this matrix B is inverted, which is possible whenever the (local) axial velocity is not equal to zero or to the speed of sound. Then the eigenvalues and eigenfunctions of $B^{-1}A$ are found using a standard QR solver. Note that due to transformation (9) the matrix $B^{-1}A$ is real for hard wall boundary conditions. Therefore, the amount of computer memory and the amount of computing time needed, will be less than for complex equations.

The numerical method was tested against analytical results for uniform flows, for which excellent agreement was found. In order to test the effects of a swirling flow, comparison with published results from Kousen[8] and Tam & Auriault[10] was made and comparison with an analytical approximation for a small solid block swirl was made. Good agreement was found. Some of the results are presented below.

Free vortex swirl

In order to test the method described above, cases published both by Kousen[8] and Tam & Auriault[10] were calculated. In fact, Tam & Auriault used the results of Kousen to test their own method. They found that their results were in agreement except for an unstable mode that was found by Tam & Auriault, but not by Kousen.

A number of cases published in references 8 and 10 were calculated and our results were found in very good agreement. Furthermore, we found that although Tam & Auriault compare their results with those of Kousen, they are considering a slightly different mean flow. Where Kousen is considering a homentropic flow, Tam & Auriault are considering a flow with constant mean density. This leads to different results as we show for a free-vortex swirl case.

The mean flow under consideration is in an annular cylinder with hub $h = 0.4$ and is described by

$$V_x = M, \quad V_\theta = \Gamma / r, \quad M = 0.3, \quad \Gamma = 0.2 . \qquad (14)$$

Tam & Auriault use a constant density

$$\rho_0 = 1 , \qquad (15)$$

whereas Kousen uses a homentropic mean flow, resulting in

$$\rho_0 = \left(1 + \Gamma^2 (\gamma - 1)\left(1 - 1/r^2\right)/2\right)^{1/(\gamma-1)} . \qquad (16)$$

The pressure distribution follows from (6) or (7), respectively.

In Figure 2 the 'acoustic' modes are shown for m = 2 and ω = -10. The spectrum for both mean flows differs slightly. Differences become more apparent near the continuum modes. This is shown in Figure 3. For the constant density mean flow, an unstable and a damped mode are found. The corresponding wave modes are α = 26.18 ± 0.239 i, which is in perfect agreement with the result from Tam & Auriault. Also, for the homentropic flow these modes are not found, which is in agreement with the result from Kousen. Since the only difference between both cases is the mean density (and resulting mean pressure), we conclude that the instability is due to an unfavourable density profile (in combination with the swirling flow). Note that the often used necessary and sufficient stability condition by Rayleigh (see, e.g., references 14 and 15) is only valid for incompressible perturbations. Although sufficient conditions for the stability of a compressible swirling flow have been found in the literature[16] these conditions do not apply in the present cases. However, it would seem that an outwardly increasing density distribution increases the stability of the flow. This is what we find here too.

The pressure component and the divergence of the velocity of the instability wave are shown in Figure 4. The pressure component is in perfect agreement with the result of Tam & Auriault. The divergence of the velocity was not given before and shows that the instability wave is not incompressible. Hence, it does not satisfy the assumption of incompressible perturbations for Rayleigh's stability criterion.

In Figure 3 also a band of continuum modes is shown for $25 \le \mathrm{Re}(\alpha) \le 32$. This band is found for both the homentropic flow and the constant mean density flow. Note that for these free vortex swirl cases no isolated (discrete) hydrodynamic modes

exist. For the constant mean density flow also two bands of non-converged modes are found. The discussion of these modes is postponed after an analytical discussion of the swirling flow problem. This analytical discussion is given to further validate the numerical method and in order to give an explanation for the non-converged modes.

Analytical description

When linearised, equations (1) − (3) can be solved algebraically for density and perturbed axial and circumferential velocities

$$\begin{aligned}
\rho &= \frac{\rho_0}{\gamma p_0} p - \frac{\rho_0}{\tilde{\omega}} \left\{ \frac{1}{\gamma p_0} \frac{\mathrm{d}p_0}{\mathrm{d}r} - \frac{1}{\rho_0} \frac{\mathrm{d}\rho_0}{\mathrm{d}r} \right\} (iu_r), \\
u_\theta &= \frac{1}{\tilde{\omega}} \left(\frac{\mathrm{d}V_\theta}{\mathrm{d}r} + \frac{V_\theta}{r} \right) (iu_r) - \frac{1}{\rho_0 \tilde{\omega}} \frac{m}{r} p, \\
u_x &= \frac{1}{\tilde{\omega}} \frac{\mathrm{d}V_x}{\mathrm{d}r} (iu_r) - \frac{1}{\rho_0 \tilde{\omega}} \alpha p,
\end{aligned} \tag{17}$$

where $\tilde{\omega}(r) = \omega + mV_\theta(r)/r + \alpha V_x(r)$. Note that the 'original' variables are used, without applying transformation (9). For the pressure and radial velocity perturbations a system of first order differential equations is found

$$\begin{aligned}
\tilde{\omega} \frac{\mathrm{d}p}{\mathrm{d}r} + \rho_0 A (iu_r) + Bp &= 0, \\
\rho_0 \tilde{\omega} \frac{\mathrm{d}(iu_r)}{\mathrm{d}r} + \rho_0 C (iu_r) - Dp &= 0,
\end{aligned} \tag{18}$$

where

$$\begin{aligned}
A &= \tilde{\omega}^2 - 2 \frac{V_\theta}{r} \left(\frac{\mathrm{d}V_\theta}{\mathrm{d}r} + \frac{V_\theta}{r} \right) \\
&\quad + \frac{V_\theta^2}{r} \left\{ \frac{1}{\gamma p_0} \frac{\mathrm{d}p_0}{\mathrm{d}r} - \frac{1}{\rho_0} \frac{\mathrm{d}\rho_0}{\mathrm{d}r} \right\}, \\
B &= \frac{V_\theta}{r} \left(\frac{2m}{r} - \frac{\rho_0 \tilde{\omega}}{\gamma p_0} V_\theta \right), \\
C &= \frac{\tilde{\omega}}{r} - \left[\frac{m}{r} \left(\frac{\mathrm{d}V_\theta}{\mathrm{d}r} + \frac{V_\theta}{r} \right) + \alpha \frac{\mathrm{d}V_x}{\mathrm{d}r} \right] + \frac{\rho_0 \tilde{\omega}}{\gamma p_0} \frac{V_\theta^2}{r}, \\
D &= \left[\frac{\rho_0 \tilde{\omega}^2}{\gamma p_0} - \left(\frac{m^2}{r^2} + \alpha^2 \right) \right].
\end{aligned} \tag{19}$$

Note that equations (17) and (18) are equivalent to the system of equations (10). From equations (17) and (18) it follows that for real eigenvalues the solution for the perturbed radial velocity is 90 degrees out of phase with the solution for the other perturbations. Moreover, when α is an eigenvalue for a hard walled duct with eigenfunction $(\rho, iu_r, u_\theta, u_x, p)$, then the complex conjugated value is also an eigenvalue having the complex conjugated eigenfunction. Hence, when the eigenvalue is real the eigenfunction $(\rho, iu_r, u_\theta, u_x, p)$ is real.

The system (18) is equivalent to a single second-order differential equation for the perturbed pressure or for the perturbed radial velocity. Here only the equation for the perturbed pressure is given

$$\begin{aligned}
&\left[AD + BC + \rho_0 \tilde{\omega} A \left(\frac{B}{\rho_0 A} \right)' - \rho_0 \tilde{\omega}^2 A \left(\frac{1}{r \rho_0 A} \right)' \right] p \\
&+ \rho_0 \tilde{\omega}^2 A \left[\frac{1}{r \rho_0 A} (rp)' \right]' = 0.
\end{aligned} \tag{20}$$

The prime again denotes differentiation with respect to radius. This equation corresponds to equation (20) of Tam & Auriault.[10] The second-order equation for the perturbed radial velocity corresponds to equation (10) of Kerrebrock.[3] In case of a uniform flow equation (20) reduces to the convected wave equation.

Small solid block swirl

The analytical description above can be used to find an analytic approximation for the spectrum of a small solid block swirling flow. This approximation can then be used for validation of the numerical method.

Consider a small solid block swirl and a constant axial flow:

$$V_\theta = \varepsilon r, \quad V_x = M. \tag{21}$$

In equation (20) all quantities of second order or higher in ε will be neglected. This may be done for

a constant density flow or for a homentropic flow. For the latter

$$\rho_0 = \left(1-\varepsilon^2(\gamma-1)\left(1-r^2\right)/2\right)^{1/\gamma-1}. \qquad (22)$$

The final approximation will be the same, as can be expected since the background flow differs only in second order in ε.

Neglecting second order effects, equation (20) reduces to a Bessel equation, having solution

$$p(r) = aJ_m(\lambda r) + bY_m(\lambda r). \qquad (23)$$

The radial wave number λ and the axial wave number α are linked by a fourth order dispersion relation for α. This means that the acoustic waves and the hydrodynamic waves are coupled. Assuming that both types of waves have well separated wave numbers the dispersion relation may be solved approximately. This yields for the acoustic modes

$$\alpha = \frac{(\omega+m\varepsilon)M}{1-M^2} \pm \sqrt{\frac{(\omega+m\varepsilon)^2}{\left(1-M^2\right)^2} - \frac{\lambda^2}{1-M^2}}, \qquad (24)$$

and for the hydrodynamic modes

$$\alpha = -\frac{\omega+m\varepsilon}{M} \pm \frac{2\varepsilon(\omega+m\varepsilon)}{M\sqrt{(\omega+m\varepsilon)^2+M^2\lambda^2}}. \qquad (25)$$

The expression for the acoustic modes is in agreement with Kerrebrock who derived it for homentropic flow.[3] However, the expression is also valid for constant density flows.

The value for λ is determined by the boundary condition, which reads for hard walls, up to first order in ε,

$$\frac{\partial p}{\partial r} = -\frac{2m\varepsilon}{r(\omega+\alpha M)}p. \qquad (26)$$

Satisfying this relation at the hub and at the duct outer radius determines a discrete set of values for λ. For the acoustic modes the value for λ can be approximated up to first order in ε. This does not hold for the hydrodynamic modes, since for the higher order radial hydrodynamic modes $\omega+\alpha M$ tends to $-m\varepsilon$. However, for the hydrodynamic modes it suffices to find λ up to zero-th order. Therefore, for the low-order radial modes the uniform flow approximation is used for the boundary condition. As the radial order increases the radial derivative term becomes more important and the boundary condition reduces to the uniform flow boundary condition.

In Figure 5 the acoustic modes are shown for M = 0.3, m = 2, ω = −10.0, h = 0.4, and ε = 0.1. The numerical results are for a constant density flow (x) and for a homentropic flow (+). These results are compared with the analytical approximation (o). The analytical approximation uses the boundary condition up to first order in ε. It is shown that the numerical results are in very good agreement with the analytical approximation. Also, the difference between a constant density flow and a homentropic flow is negligible.
In Figure 6 one branch of the hydrodynamic modes is presented for the same conditions as Figure 5. Again, numerical results for constant density and homentropic flow coincide. The analytical approximation is very close.

The analytical approximation in Figure 6 yields one extra mode at the beginning of the sequence. This mode must be neglected, since it is no physical solution. The explanation for this is as follows. The acoustic modes are pressure dominated. The corresponding n-th radial eigenfunction has $n-1$ zeros for the pressure component. The hydrodynamic modes are velocity dominated. For these modes the n-th radial eigenfunction has $n-1$ zeros for the radial velocity component. The extra mode in the analytical approximation of the hydrodynamic modes shown in Figure 6 has no zeros in the pressure component of the eigenfunction. This mode, however, does not correspond with a physical solution for the radial velocity component. Therefore, this mode is not physical and must be neglected. It is also not found by the numerical method.

In Figure 7 the acoustic modes are shown for an increased solid block swirl of ε = 0.5. This condition corresponds to the results of Kousen[8] and Tam & Auriault[10] for solid block swirl. Since the swirl is not small anymore, the analytical approximation differs from the numerical results. Also the results for the constant density flow and the homentropic flow differ now. Hence, in general different density profiles generate different spectra for equal swirl distributions.

Continuum modes and local cluster condition

So far a number of different modes were encountered. Acoustic modes both for free vortex and solid block swirl, instability waves for a constant density free vortex swirl, hydrodynamic modes for solid block swirl, and continuum modes for free vortex swirl. In this section we discuss the poor convergence of the continuum modes by the numerical method and the question of existence of the hydrodynamic modes.

The continuous spectrum was analysed by Case for an inviscid plane Couette flow[17] and for an idealised atmosphere.[4] Here we consider its existence for a circular or annular geometry containing an arbitrary flow. The continuous spectrum is given by the condition

$$\tilde{\omega}(r) = \omega + mV_\theta(r)/r + \alpha V_x = 0 \ . \tag{27}$$

In this case the coefficients of the radial derivatives in equation (18) become zero.

Suppose that $\tilde{\omega}(r_c) = 0$, while $\tilde{\omega}'(r_c) \neq 0$. r_c is the radial position of the so called critical layer. Defining a new variable $s = r - r_c$ equation (20) can be expanded in a series around the critical layer $s = 0$. Using a Frobenius series expansion for the perturbed pressure around the critical layer,[18]

$$p(s) = s^n \sum_{i=0}^{\infty} p_i s^i , \tag{28}$$

it follows from equation (20) that (unless the swirl is a homentropic, free vortex swirl)

$$n_{1,2} = \frac{1}{2} \pm \sqrt{\frac{1}{4} - \Lambda/(\omega_c')^2} , \tag{29}$$

where

$$\begin{aligned} \Lambda = {} & 2\alpha_c \frac{V_\theta}{r_c} \left\{ \alpha_c \left(\frac{\mathrm{d}V_\theta}{\mathrm{d}r} + \frac{V_\theta}{r_c} \right) - \frac{m}{r_c} \frac{\mathrm{d}V_x}{\mathrm{d}r} \right\} \\ & - \left(\frac{m^2}{r_c^2} + \alpha_c^2 \right) \frac{V_\theta^2}{r_c} \left\{ \frac{1}{\gamma p_0} \frac{\mathrm{d}p_0}{\mathrm{d}r} - \frac{1}{\rho_0} \frac{\mathrm{d}\rho_0}{\mathrm{d}r} \right\}, \end{aligned} \tag{30}$$

$$\omega_c' = \frac{m}{r_c} \left(\frac{\mathrm{d}V_\theta}{\mathrm{d}r} - \frac{V_\theta}{r_c} \right) + \alpha_c \frac{\mathrm{d}V_x}{\mathrm{d}r} , \tag{31}$$

and

$$\alpha_c = -\frac{1}{V_x} \left(\omega + \frac{m}{r_c} V_\theta \right) \tag{32}$$

Note that all these quantities are evaluated at the critical layer. ω_c' is the derivative of $\tilde{\omega}(r)$ at the critical layer and α_c is the axial wave number corresponding to the continuum mode at the critical layer.

In general, the continuous spectrum consists of a strip of values α_c. Only in case of a solid block swirl with constant axial flow, of which a uniform flow is a special case, this strip reduces to a single point.

From equations (17) and (18) the behaviour of the other variables around the critical layer can be found:

$$\begin{aligned} p(s) &= \gamma_1(s) s^{n_1} + \gamma_2(s) s^{n_2} , \\ u_r(s) &= \gamma_3(s) s^{n_1} + \gamma_4(s) s^{n_2} , \\ u_\theta(s) &= \gamma_5(s) s^{n_1 - 1} + \gamma_6(s) s^{n_2 - 1} , \\ u_x(s) &= \gamma_7(s) s^{n_1 - 1} + \gamma_8(s) s^{n_2 - 1} , \\ \rho(s) &= \frac{\rho_0}{\gamma p_0} p(s) + \gamma_9(s) s^{n_1 - 1} + \gamma_{10}(s) s^{n_2 - 1} . \end{aligned} \tag{33}$$

The functions γ_i are regular functions in the entire radial domain. For a homentropic flow $\gamma_9 = \gamma_{10} = 0$.

In case $\Lambda/(\omega_c')^2 < 1/4$ at least one of the solutions for u_θ and u_x and possibly ρ becomes infinite at the critical layer. When $\Lambda/(\omega_c')^2 < 0$ all perturbations have one infinite solution.

In case

$$\Lambda/(\omega_c')^2 > 1/4 \tag{34}$$

all solutions remain bounded. However, now all solutions oscillate infinitely fast when approaching the critical layer.

In all cases it is always possible to satisfy the boundary conditions and, therefore, α_c is part of the continuous spectrum for all radial positions.

Since the eigenfunctions corresponding to the continuous spectrum are singular, it is very hard to approximate them numerically on a finite grid. Therefore, the convergence of the continuous spectrum may be slow. In Figure 8 the continuous spectrum for a constant density free vortex is shown. In this case $\Lambda/(\omega_c')^2 < 0$ so that all perturbations have an infinite solution at the critical layer. This explains the bands of non-converged eigenvalues. Since the eigenfunctions are determined by the position of the critical layer, the number of modes that is found in the range of the continuous spectrum depends linearly on the number of grid points.

When condition (34) holds not only a continuous spectrum exists, but also one or two sets hydrodynamic modes exist. A loose explanation is that in this case the continuous spectrum consists of infinitely oscillating eigenfunctions. Perturbing the spectrum slightly then allows for discrete eigenvalues having oscillating eigenfunctions that can satisfy the boundary condition. A more detailed analysis shows that in this case the eigenvalue can only be real. Since perturbing the eigenvalue inside the strip of continuous eigenvalues yields again an eigenvalue of the continuous spectrum, the discrete eigenvalues can only cluster towards the edges of the continuous spectrum. Therefore, in order to have a set of hydrodynamic cluster modes, the cluster condition (34) should be satisfied at either the hub position or the outer radius position. This means that depending on the mean flow, zero, one or two sets of hydrodynamic modes may occur.

For a homentropic flow having constant axial velocity and a combination of a solid block and a free vortex swirl, condition (34) reduces to the cluster condition found by Golubev & Atassi who derived it in the thin annulus approximation.[9]

For a uniform density, free vortex swirl without axial shear $\Lambda < 0$ and no hydrodynamic modes exist, see Figures 3 and 4. Similarly, for an homentropic solid block swirl without axial shear $\Lambda = +\infty$ and two sets of hydrodynamic modes exist of which Figure 6 shows one set.

Conclusions

In this paper a numerical method for the solution of the eigenvalues and eigenfunctions of a general non-uniform flow was presented. This method was validated against uniform flow and swirling flow results. Agreement was excellent for acoustic modes, hydrodynamic modes and instability modes. The continuum modes are badly resolved, since their eigenfunctions show non-regular behaviour at the critical layer.

Since the method does not assume a homentropic flow, we were able to compare results for a homentropic flow with results for a constant density flow. Although the eigenvalues for both cases show the same patterns, small differences in the actual values are obtained. Of interest is that the density distribution may affect the stability of the swirling flow. Therefore, one should be careful in applying Rayleigh's stability criterion (for incompressible flows) to these flows.

The analysis of the small solid block swirl showed that the acoustic eigenvalues are changed in first order of the swirl. Also two sets of hydrodynamic modes appear that cluster towards the continuum. The approximate solution for the small solid block swirl was used to validate the numerical method.

Finally the existence of hydrodynamic modes was investigated. It was shown that whenever the continuum modes have infinitely oscillating behaviour at the hub and / or outer radius hydrodynamic modes clustering towards the edge of the continuum may exist. This means that in general there may be zero, one, or two sets of hydrodynamic modes.

Acknowledgement

This work was partly performed in the 'Turbonoise CFD' project, one of the Key Action Aeronautics research projects in the Growth Programme of the European Community.

References

1. Nijboer, R.J., and Sijtsma, P., "Sound diffraction by the splitter of a turbofan engine", NLR-TP-99133, paper presented at

the 6th International Congress on Sound and Vibration (Lyngby, Denmark), 1999.
2. Tyler, J.M., and Sofrin, T.G., "Axial flow compressor studies", *SAE Transactions*, Vol. 70, 1962, pp. 309 – 332.
3. Kerrebrock, J.L., "Small disturbances in turbomachine annuli with swirl", *AIAA Journal,* Vol. 15, 1977, pp. 794 – 803.
4. Case, K.M., "Stability of an idealized atmosphere. I. Discussion of results", *The Physics of Fluids*, Vol. 3, 1960, pp. 149 – 154.
5. Goldstein, M.E., "Scattering and distortion of the unsteady motion on transversely sheared mean flows", *Journal of Fluid Mechanics*, Vol. 91, 1979, pp. 601 – 632.
6. Golubev, V.V., and Atassi, H.M., "Aerodynamic and acoustic response of a blade row in unsteady swirling flow", *Proceedings of the first joint CEAS/AIAA Aeroacoustics conference* (Munich, Germany), 1995, pp. 167 – 176.
7. Kousen, K., "Eigenmode analysis of ducted flows with radially dependent axial and swirl components", CEAS/AIAA Paper 95-160, 1995.
8. Kousen, K., "Pressure modes in ducted flows with swirl", AIAA Paper 96-1679, 1996.
9. Golubev, V., and Atassi, H., "Acoustic-vorticity waves in swirling flows", *Journal of Sound and Vibration*, Vol. 209, 1998, pp. 203 – 222.
10. Tam, C., and Auriault, L., "The wave modes in ducted swirling flows", *Journal of Fluid Mechanics*, Vol. 371, 1998, pp. 1 – 20.
11. Myers, M.K., "On the acoustic boundary condition in the presence of flow", *Journal of Sound and Vibration*, Vol. 71, 1980, pp. 429 – 434.
12. Kerner, W., Lerbinger, K., Gruber, R., and Tsunematsu, T., "Normal mode analysis for resistive cylindrical plasmas", *Computer Physics Communications*, Vol. 36, 1985, pp. 225 – 240.
13. Nijboer, R.J., V.d. Holst, B., Poedts, S., and Goedbloed, J.P., "Calculating magnetohydro-dynamic flow spectra", *Computer Physics Communications*, Vol. 101, 1997, pp. 39 – 52.
14. Chandrasekhar, S., *Hydrodynamic and Hydromagnetic Stability*, Oxford University Press, 1961.
15. Howard, L.N., and Gupta, A.S., "On the hydrodynamic and hydromagnetic stability of swirling flows", *Journal of Fluid Mechanics*, Vol. 14, 1962, pp. 463 – 476.
16. Lalas, D.P., "The 'Richardson' criterion for compressible swirling flows", *Journal of Fluid Mechanics*, Vol. 69, 1975, pp. 65 – 72.
17. Case, K.M., "Stability of inviscid plane Couette flow", *The Physics of Fluids*, Vol. 3, 1960, pp. 143 – 148.
18. Bender, C.M., and Orszag, S.A., *Advanced Mathematical Methods for Scientists and Engineers*, Springer-Verlag New York, 1999.

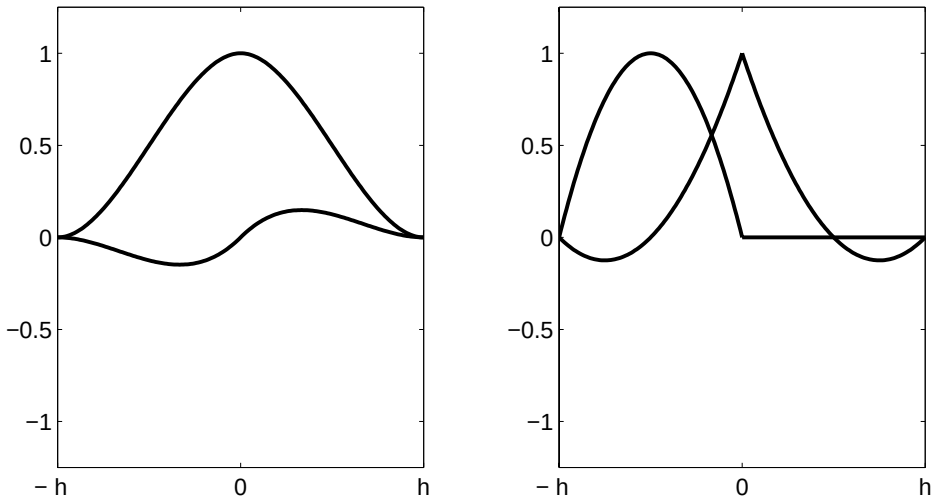

Figure 1 Basis functions. Left: cubic element and its derivative; right: two types of quadratic elements.

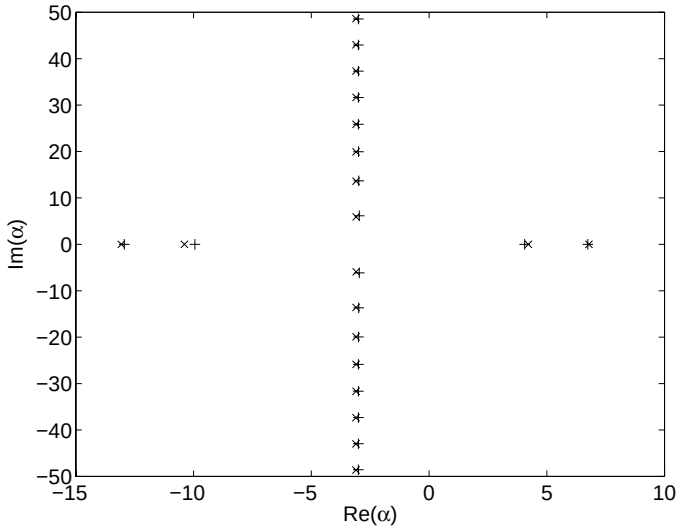

Figure 2 Comparison of acoustic modes for free vortex swirl: homentropic flow (+) and constant density flow (×).

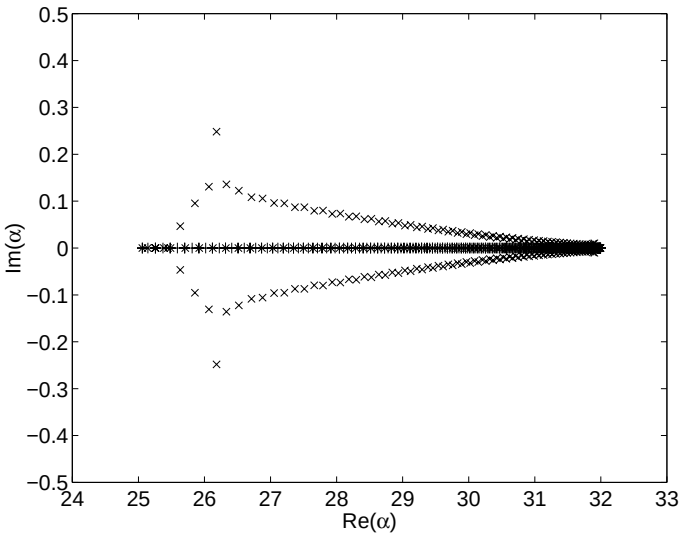

Figure 3 Comparison of continuum for free vortex swirl: homentropic flow (+) and constant density flow (×).

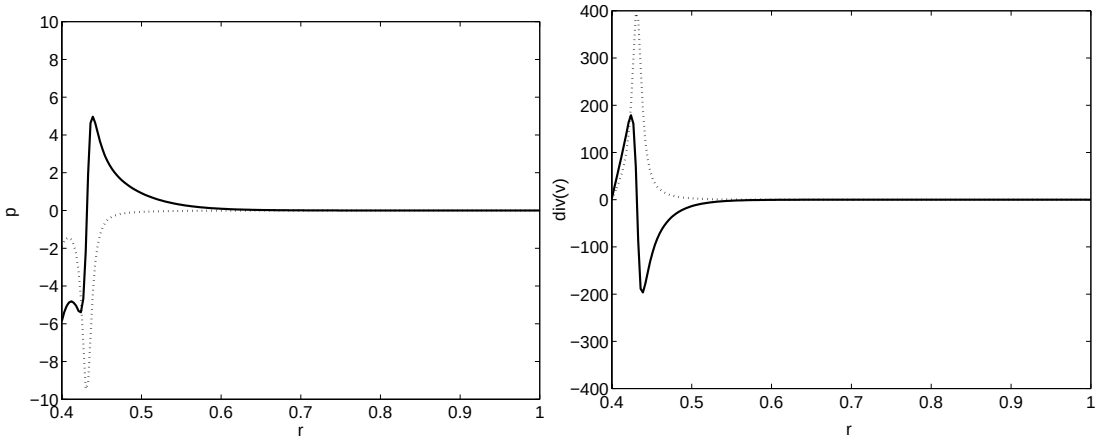

Figure 4 Eigenfunction of instability wave: pressure (left) and divergence (right). Solid line: real part; dotted line: imaginary part.

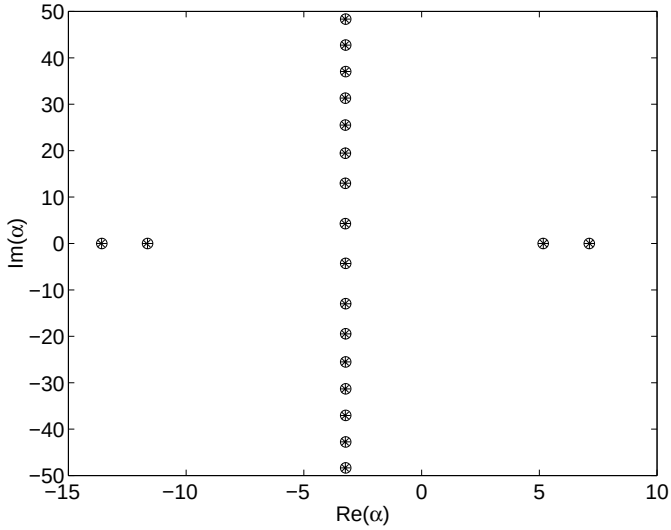

Figure 5 Acoustic modes for a small solid block swirl (ε = 0.1): homentropic flow (+), constant density flow (×), analytical approximation (o).

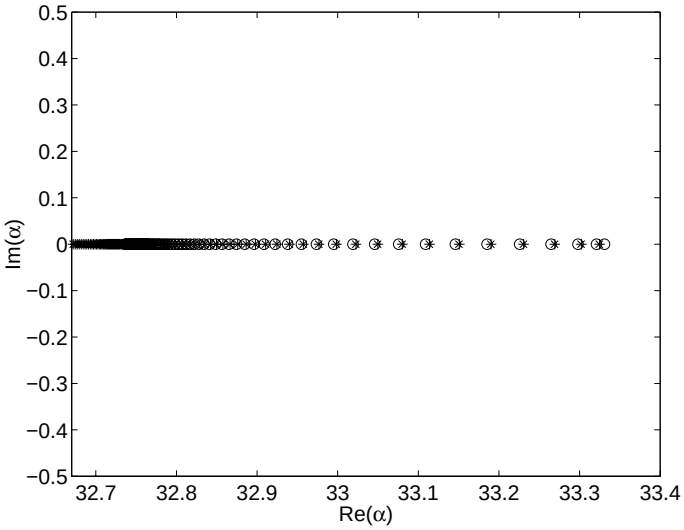

Figure 6 Hydrodynamic modes for a small solid block swirl (ε = 0.1): homentropic flow (+), constant density flow (×), analytical approximation (o).

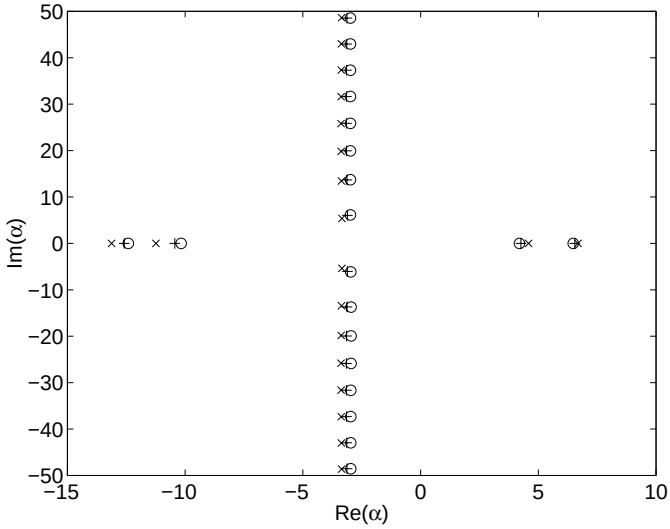

Figure 7 Acoustic modes for a solid block swirl (ε = 0.5): homentropic flow (+), constant density flow (×), analytical approximation (o).

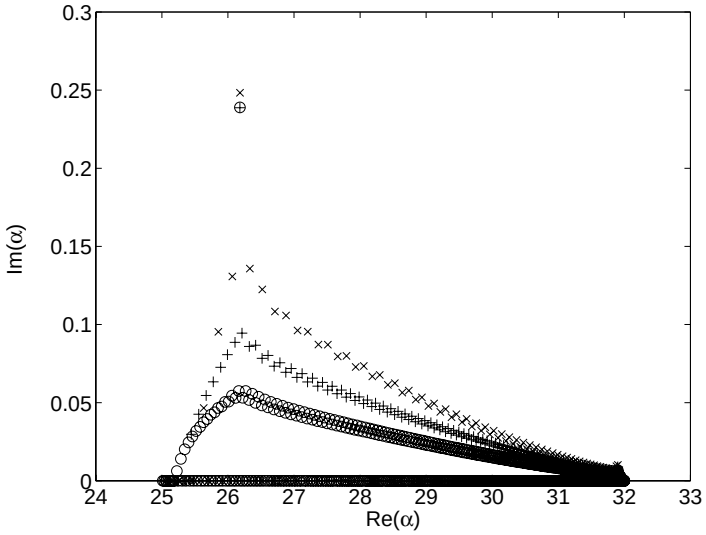

Figure 8 Grid refinement for constant density free vortex swirl continuum modes: N = 51 (×), N = 101 (+), N = 201 (o).